

TOPOGRAPHY BASED SURFACE AGE COMPUTATIONS FOR MARS: A STEP TOWARD THE FORMAL PROOF OF MARTIAN OCEAN RECESSION, TIMING AND PROBABILITY. G. Salamunićar¹ and Z. Nežić², ¹AVL-AST d.o.o., Av. Dubrovnik 10/II, HR-10020 Zagreb-Noví Zagreb, Croatia, Europe, gsc@ieee.org, ²Trg kralja Zvonimira 20, HR-48000 Koprivnica, Croatia, Europe, Zdravko.Nezic@ieee.org.

Introduction: Large body of work on the impact crater statistics was already done, as e.g. described by Neukum [1], where Hatmann's model from 1981 and Neukum's model from 1981 and 1983 were compared, and where Cratering Chronology Diagrams were shown in log/log scale, showing Cumulative Crater Frequency ($N \text{ km}^{-2}$) as a function of Age (years) for some particular crater diameter. However, recently it was presented that this [2], according to the Mathematical Theory of Stochastic Processes (MTSP), is only one possible representation of bombardment of lunar/planetary surface modeled as stochastic process in the Mathematical Statistics Theory (MST) domain [3]. Basic idea is that there is more than one representation in the MST domain of the same stochastic process modeled according to MTSP, where each one can provide us with new information about some lunar/planetary body [3]. First work in this new field [3] resulted in representation of crater statistics in the form of the Topography Profile Diagrams (TPDs) [4, 5, 6]. They show correlation hardly explainable by anything other than an ancient ocean, offering an opportunity to prove existence of Martian ocean, if it will be possible to prove that nothing else could cause such correlation [7]. This is particularly interesting because after the initial proposal of Contact 1 and 2 [8], many other indications of oceanic phases on Mars were also proposed, for example episodic water inundations in the northern plains [9] caused by Tharsis and Elysium-triggered catastrophic outflows [10, 11] that ponded in the northern plains to form large water bodies, aptly explained by the MEGAOUTFLO hypothesis [12, 13], possible hydroisostatic influences on the collective geometry of strandline features [14], cracking of the cryosphere by dike injection and subsequent release of water from a confined aquifer that can take place fast enough to form an ocean [15], etc.

Surface Age Computations (SAC): Additional application of MTSP in the Lunar and Planetary Science (LPS) domain is shown by proposal of SAC algorithm [16]. For area of $x \text{ [km}^2\text{]}$ and n craters, density of craters is defined as $d=n/x$. However, density of craters for some point can be defined in more than one way. The proposed algorithm is as follows. A circle is defined with center in the point, large just enough to contain m craters. Then we can define density of craters as $m/(r^2 \pi)$. In order to have the same resolution, no

matter how many craters there are in some data-set, we can define m as e.g. $s/256$, as it is also proposed in [16], where s is the total number of craters in some data-set. Results are shown in Fig. 1-4.

Topography based SAC (SACT): Additionally, we can divide density of craters for each point with the average density of craters for point's elevation, which can easily be read from TPDs for each altitude. Accordingly, age is not computed as relative to the average surface age of the whole planet, like in the SAC case (age_1), but as relative to the average surface age at the corresponding altitude (age_2). Results are shown in Fig. 5-8. We can note that the largest volcanoes, as well as the regions possibly covered by north and south polar caps, are inside the regions that are found this way. This is particularly interesting because it shows how influence of past lava flows and polar caps on craters statistics can be measured, i.e. how using crater statistics can help us reconstruct with certain probability past lava-flows and polar caps.

Conclusion: SACT algorithm shows additional applications of MTSP in LPS domain. Its use in reconstruction of past lava-flows and polar caps with other techniques currently in use is one possible application, while results can also be used together with TPDs regarding further search for proof of an ancient ocean.

References: [1] Neukum G. (1988) *Workshop on Mars Sample Return Science*, 128-129. [2] Salamunićar G. (2002) *34th COSPAR*, Abstract #01766. [3] Salamunićar G. (2004) *Adv. Space Res.*, in press. [4] Salamunićar G. (2003) *LPS XXXVIII*, Abstract #1403. [5] Nežić Z. and Salamunićar G. (2003) *LPS XXXVIII*, Abstract #1409. [6] Nežić Z. and Salamunićar G. (2003) *LPS XXXVIII*, Abstract #1415. [7] Salamunićar G. (2003) *6th Int. Conf. on Mars*, Abstract #3187. [8] Parker T. J. et al. (1989) *Icarus*, 82, 111-145. [9] Fairén A. G. et al. (2003) *Icarus*, 165, 53-67. [10] Dohm J. M. et al. (2001) *JGR*, 106, 32943-32958. [11] Fairén A. G. et al. (2003) *LPS XXXVIII*, Abstract #1093. [12] Baker V. R. et al. (1991) *Nature*, 352, 589-594. [13] Baker V. R. et al. (2000) *LPS XXXI*, Abstract #1863. [14] Leverington D. W. et al. (2003) *LPS XXXVIII*, Abstract #1282. [15] Wilson L. and Head J. W. (2003) *LPS XXXVIII*, Abstract #1186. [16] Salamunićar G. (2003) *LPS XXXVIII*, Abstract #1421.

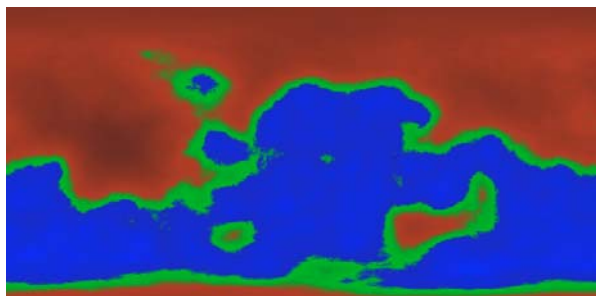


Figure 1: Surface age computations for 9496 craters and surface age as background: $age_1 < 50\%$ (red), $50\% < age_1 < 100\%$ (green) and $age_1 > 100\%$ (blue).

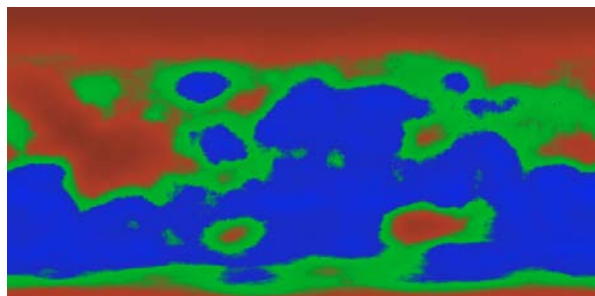


Figure 2: Surface age computations for 22044 craters and surface age as background: $age_1 < 50\%$ (red), $50\% < age_1 < 100\%$ (green) and $age_1 > 100\%$ (blue).

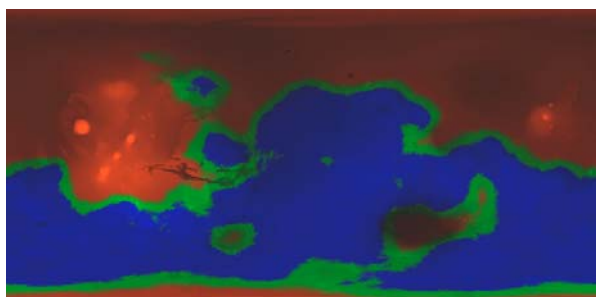


Figure 3: Surface age computations for 9496 craters and topography as background: $age_1 < 50\%$ (red), $50\% < age_1 < 100\%$ (green) and $age_1 > 100\%$ (blue).

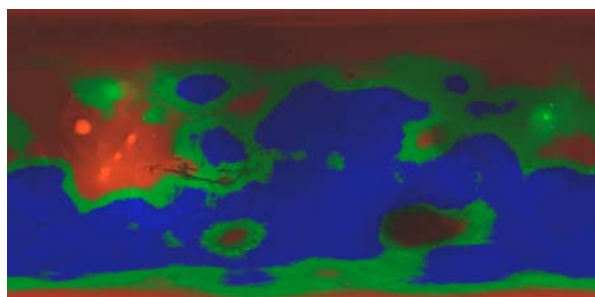


Figure 4: Surface age computations for 22044 craters and topography as background: $age_1 < 50\%$ (red), $50\% < age_1 < 100\%$ (green) and $age_1 > 100\%$ (blue).

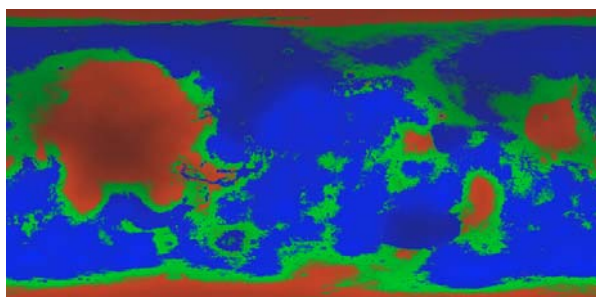


Figure 5: Topography based surface age computations for 9496 craters and surface age as background: $age_2 < 50\%$ (red), $50\% < age_2 < 100\%$ (green) and $age_2 > 100\%$ (blue).

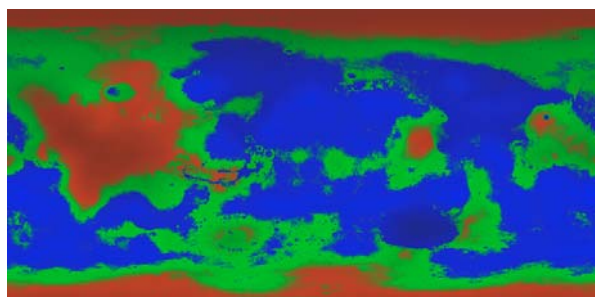


Figure 6: Topography based surface age computations for 22044 craters and surface age as background: $age_2 < 50\%$ (red), $50\% < age_2 < 100\%$ (green) and $age_2 > 100\%$ (blue).

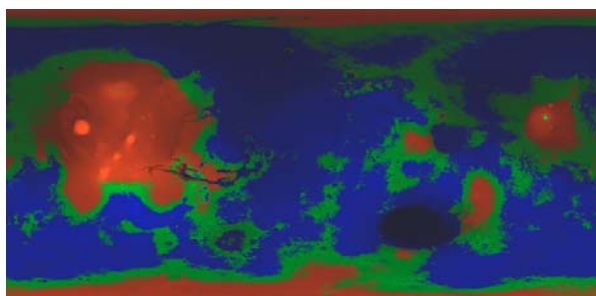


Figure 7: Topography based surface age computations for 9496 craters and topography as background: $age_2 < 50\%$ (red), $50\% < age_2 < 100\%$ (green) and $age_2 > 100\%$ (blue).

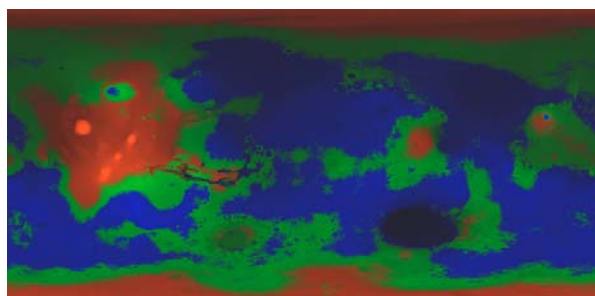


Figure 8: Topography based surface age computations for 22044 craters and topography as background: $age_2 < 50\%$ (red), $50\% < age_2 < 100\%$ (green) and $age_2 > 100\%$ (blue).